# Designing Thiophene-Based Azomethine Oligomers with Tailored Properties: Self-assembly and Charge Carrier Mobility

Nataliya Kiriy,[†] Vera Bocharova,[‡] Anton Kiriy,*[,‡] Manfred Stamm,[‡] Frederik C. Krebs,[§] and Hans-Juergen Adler[†]

*Institut für Makromolekulare Chemie und Textilchemie, Mommsenstrasse 13, 01062 Dresden, Germany, Institut für Polymerforschung Dresden, Hohe Strasse 6, 01069 Dresden, Germany, and The Danish Polymer Centre, RISØ National Laboratory, P.O. Box 49, DK-4000 Roskilde, Denmark*

*Received February 27, 2004. Revised Manuscript Received April 29, 2004*

This paper describes synthesis and characterization of two thiophene-based azomethines designed to optimize solubility, self-assembly, and charge carrier mobility. We found that incorporation of azomethine and amide moieties in the α,ω-position, and hexyl chains in the β-position of the quaterthiophene, considerably improves the self-assembly properties without suppression of solubility. Self-assembly of azomethine oligomers with (QT-amide) and without amide moieties (QT-aniline) were monitored by UV−vis, XRD, and AFM. Although no changes in the UV−vis spectrum of QT-aniline is observed upon addition of hexane to the solution in THF, the addition of hexane to QT-amide solution induces a red shift of $\lambda_{max}$ and appearance of fine structure believed to be vibronic in nature. The concentration dependence of the solvatochromism gives strong support for the *inter*molecular origin of this effect and clearly indicates that the planarization of the oligomer backbone is forced by the aggregation. Although, no clear signs of the molecular order for various QT-aniline films are observed by AFM, UV−vis, and XRD measurements, the QT-amide film after the annealing at 180 °C displays important molecular and macroscopic orientations. The sum of charge carrier mobilities as determined by pulse-radiolysis time-resolved microwave conductivity (PR-TRMC) technique for QT-aniline was shown to be below the detectable limit; the mobility of QT-amide was determined to be $1 \times 10^{-2}$ cm$^2$ V$^{-1}$ s$^{-1}$, which is comparable with the mobilities of the best organic semiconductors. All these significant differences in properties of related compounds can be attributed to the hydrogen bonding between QT-amide molecules responsible for the observed self-assembly.

## Introduction

Over the past decade π-conjugated thiophene-based oligomers have generated considerable attention because of their possible applications in light-emitting diodes, lasers, field-effect transistors (FET), and photovoltaic cells.[1] Most of unsubstituted oligothiophenes (OTs) are insoluble, which suppresses their potential industrial utility.[2] The high charge carrier mobility and poor solubility of OTs originate from the fundamental property of π-conjugated systems to pack efficiently into stacks.[3] Therefore, the solubility and the charge carrier mobility, in many cases, represent mutually "antagonistic" properties. It was previously shown that attempts to improve the solubility by incorporation of substituents in the aromatic backbone in the β-position usually breaks the conjugation between adjacent oligothiophene molecules and, hence, diminishes their electronic properties.[4a,b] On the other hand, insertion of some mesogenic groups,[4c] aimed to improve a molecular order, as a rule decreases the solubility. Garnier at al.[4a,d] have introduced a new molecular engineering approach to design organic semiconductors with desired self-assembly properties through the incorporation of mesogenic groups in the α,ω-position of the aromatic backbone of sexithiophene. Newly designed systems showed an excellent ability to form extended crystalline structures and good charge transport properties, but still displayed poor solubility. Recently, Feringa at al.[5]

* To whom correspondence should be addressed. E-mail: kiriy@ipfdd.de. Tel: +49-351-4658-294. Fax: +49-351-4658-284.
[†] Institut für Makromolekulare Chemie und Textilchemie.
[‡] Institut für Polymerforschung Dresden.
[§] RISØ National Laboratory.

(1) Skotheim, T. A.; Elsenbaumer, R. L.; Reynolds, J. R. *Handbook of Conducting Polymers*; Marcel Dekker: New York, 1998.
(2) Dimitropoulos, C. D.; Malenfant, P. R. L. *Adv. Mater.* **2002**, *14*, 99.
(3) Tsuzuki, S.; Honda, K.; Azumi, R. *J. Am. Chem. Soc.* **2002**, *124*, 12200.
(4) (a) Garnier, F.; Yassar, A.; Hajlaoui, R.; Horowitz, G.; Deloffre, F.; Servet, B.; Ries, S.; Alnot, P. *J. Am. Chem. Soc.* **1993**, *115*, 8716. (b) Videlot, C.; Ackermann, J.; Blanchard, P.; Raimundo, J.-M.; Frere, P.; Allain, M.; de Bettignies, R.; Levillain, E.; Roncali, J. *Adv. Mater.* **2003**, *15*, 306. (c) Bader, M. M.; Custelcean, R.; Ward, M. D. *Chem. Mater.* **2002**, *15*, 616. (d) Horowitz, G.; Bachet, B.; Yassar, A.; Lang, P.; Demanze, F.; Fave, L.-L.; Garnier, F. *Chem. Mater.* **1995**, *7*, 1337. Katz, H.; Lovinger, A. J.; Laquindanum, J. G. *Chem. Mater.* **1998**, *10*, 457. Wegewijs, B.; Haas, M. P.; de Leeuw, D. M.; Wilson, R.; Sirringhaus, H. *Synth. Met.* **1999**, *101*, 534. Haas, M. P.; van der Laan, G. P.; Wegewijs, B.; de Leeuw, D. M.; Bäuerle, P.; Rep, D. B. A.; Fichou, D. *Synth. Met.* **1999**, *101*, 524.

10.1021/cm049688v CCC: $27.50 
Published on Web 08/04/2004

**Scheme 1. Synthesis of Thiophene-Based Azomethine Oligomers**

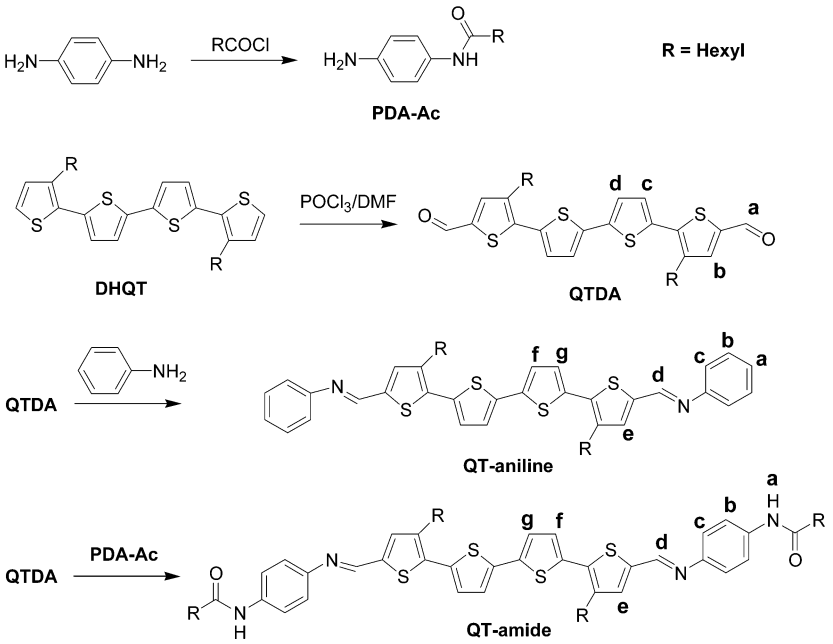


have described a range of OTs with urea moieties in the α,ω-position of the backbones. Due to the combination of hydrogen bonding and π-stacking interactions these compounds can self-assemble into long one-dimensional structures. Although such a molecular organization significantly improves the charge transport inside the stacks, these OTs, again, appear to be poorly soluble in usual organic solvents.[6]

Aromatic polyazomethines constitute a readily accessible class of π-conjugated polymers with useful optoelectronic properties.[7] They can be produced in mild conditions from easily available diamines and dialdehydes. One of the most straightforward ways to incorporate oligothiophene moiety into polyazomethine structure is to use thiophene-based dialdehydes, available by the Vilsmeier−Haack formylation.[8] The resulting polyazomethines are only partially soluble in the entire state, but can be dissolved in organic solvents after complexation with Lewis acids.[9] The latter procedure can, however, lead to doping of polyazomethines that is undesirable for some applications, such as organic FET. That is why development of new conjugated aromatics that possess a good solubility in the pristine state and good charge carrier mobilities is still a valuable goal.

By following the above-mentioned ideas, we designed a new thiophene-based azomethine oligomer that contained (a) alkyl groups in the β-position of the oligothiophene backbone to derive the solubility and (b) azomethine and amide moieties to force self-assembling in the desired way through hydrogen bonding and dipole−dipole interactions (Char 1). The idea was to use the ability of the amide group to form strong hydrogen bonds in nonpolar solvents and in the solid state, but can be easily broken in the presence of polar solvents. Thus, at the stage of dissolution and deposition, when the solubility is important, the hydrogen bonding can be "switched off" simply by adding polar solvents and then, after the removal of polar additives, the self-assembly can be "switched on". To simplify the synthesis, we applied a modular approach that allowed us to produce a number of related compounds with systematic variation of the substitution pattern through the Schiff condensation of properly substituted and easily available building blocks through symmetric synthesis. Thus, properties of resulting materials, including optical, electrical, and self-assembly, can be tuned by the incorporation of appropriate groups in starting building blocks.[7] Here we describe synthesis, aggregation, and charge mobility of two related thiophene-based azomethines with and without the amide moiety (Scheme 1). We further address the questions of how the aggregation and the charge carrier mobility depend on the structure.

## Results and Discussion

**Synthesis and Characterization.** The synthesis is based on the condensation of dihexylquaterthiophene dialdehyde (QTDA), produced from easily available dihexylquaterthiophene[10] by Vilsmeier−Haack formulation, with corresponding amines: heptanoic acid (4-aminophenyl)amide (PDA-Ac), and aniline (Scheme 1).

PDA-Ac was synthesized in moderate yield by acylation of paraphenylene using stoichiometric amounts of the reagent. The Schiff bases were obtained in high yield and could be separated by filtration and purified by

(5) Rep, D. B. A.; Roelfsema, R.; van Esch, J. H.; Schoonbeek, F. S.; Kellogg, R. M.; Feringa, B. L.; Palstra, T. T. M.; Klapwijk, T. M. *Adv. Mater.* **2000**, *12*, 563. Gesquiere, A.; de Feyter, S.; de Schryver, F. C.; Schoonbeek, F. S.; Kellogg, R. M.; Feringa, B. L. *Nano Lett.* **2001**, *1*, 201.

(6) Schoonbeek, F. S.; van Esch, J. H.; Wegewijs, B.; Rep, D. B. A.; Haas, M. P.; Klapwijk, T. M.; Kellogg, R. M.; Feinga, B. L. *Angew. Chem.* **1999**, *111,* 1486.

(7) Yang, C. J.; Jenekhe, S. A. *Macromolecules* **1995**, *28*, 1180. D′Alelio, G. F. *Encycl. Polym. Sci. Technol.* **1969**, *10*, 659. Morgan, P. W.; Kwolek, S. L.; Pietcher, T. C. *Macromolecules* **1987**, *20*, 729.

(8) MacEachern, A.; Soucy, C.; Leitch, L. C.; Arnason, J. T.; Morand, P. *Tetrahedron* **1988**, *44*, 2403. Müller, H.; Petersen, J.; Strohmaier, R.; Gompf, B.; Eisenmenger, W.; Vollmer, M. S.; Effenberger, F. *Adv. Mater.* **1996**, *8*, 733.

(9) Yang, C. J.; Jenekhe, S. A. *Chem. Mater.* **1991**, *3*, 878.

(10) Herrema, J. K.; Wildeman, J.; van Bolhius, F.; Hadziioannou, G. *Synth. Met.* **1993**, *60*, 239.

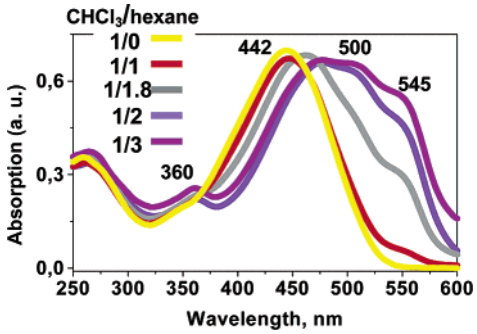


**Figure 1.** Solvent-dependent UV−vis absorption spectra of QT-amide at constant oligomer concentration (0.01 g/L) and at different chloroform−hexane ratio (from 1/0 to 1/3, v/v). Spectra were recorded 15 min after the addition of hexane.

crystallization. The structures of QT-aniline (the adduct of QTDA and aniline) and QT-amide (the adduct of QTDA and PDA-Ac) were confirmed by analysis of NMR, IR, and UV−vis spectra. QT-aniline (melting point (mp) 111.8 °C) displays high solubility in organic solvents (such as chloroform and THF), whereas QT-amide (mp 202 °C) is poorly soluble in chloroform, but is highly soluble in THF or in chloroform-methanol mixture (5−10 vol % of methanol).

**Solution Behavior.** The aggregation behavior of QT-amide and QT-aniline was studied using UV−vis spectroscopy, monitoring the changes in the $\pi \rightarrow \pi^*$ transition arising from conformational transitions of oligomer backbones. In THF QT-amide and QT-aniline show similar broad absorption spectra with $\lambda_{max} = 442$ and 432 nm, respectively, indicative of random twisted conformations. No change of the UV−vis spectra was observed upon addition of hexane to QT-aniline solution in THF. In contrast, a stepwise addition of hexane to QT-amide solution in THF induces a gradual red shift of $\lambda_{max}$ to about 500 nm and the appearance of the fine vibronic structure (shoulders at 360 and 545 nm), that reflects planarization of the backbone (Figure 1).[11]

Similar transformations of absorption spectra occurred in a chloroform-hexane mixture that was recently monitored for polyalkyl thiophenes (PATs).[12] It was shown that reconformation of PATs is an *intra*molecular process independent of the polymer concentration (the concentration was varied within 2 orders of magnitude). Figure 2 shows the evolution of the UV−vis spectra for QT-amide upon increasing the oligomer concentration at a constant chloroform/hexane ratio (1/2). We found no change in the UV−vis spectra at low QT-amide concentrations (0.001 to 0.005 g/L). When the concentration of QT-amide reaches a value of 0.01 g/L the UV−vis spectra displays a strong dependence on the oligomer

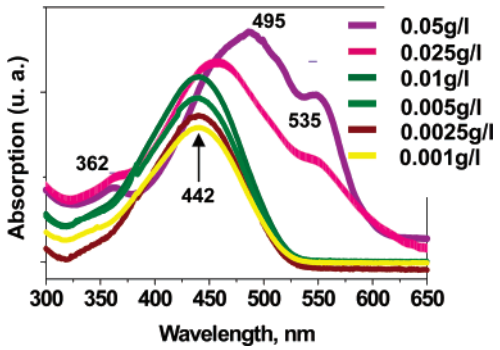


**Figure 2.** Concentration-dependent UV−vis absorption spectra of QT-amide at constant chloroform−hexane ratio 1/2 (v/v) (a).

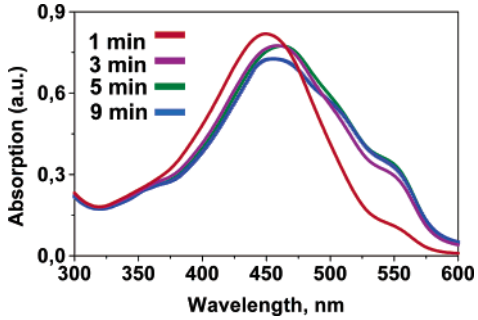


**Figure 3.** Time-dependent UV−vis absorption spectra of QT-amide at constant chloroform−hexane ratio 1/1.9 (v/v) and constant QT-amide concentration (0.02 g/L).

concentration. Such a transformation resembles the process that occurs during the change from a good to a poor solvent (Figure 1), and reflects the transition from a twisted to a more planar conformation. The concentration dependence of the solvatochromism gives strong support for the *inter*molecular origin of this effect and clearly indicates that a planarization of the oligomer backbone is induced by the aggregation. All of the spectra shown in Figures 1 and 2 were recorded 15 min after the addition of hexane and present an equilibrium state. Figure 3 shows the transformation of the QT-amide spectra recorded in time with a fixed chloroform-hexane ratio (1/1.9). The spectra obtained after addition of hexane and stirring for 1 min resemble the spectra obtained for QT-amide recorded in pure chloroform ($\lambda_{max} = 450$ nm, Figure 3). When recording the spectra after 9 min a large red shift (to $\lambda_{max} = 462$ nm) is observed. The spectrum also develop shoulders around 360 and 550 nm.

Previously, we showed that the changes in conformation of considerably longer PAT molecules is an *intra*molecular process that takes place within a few seconds after addition of a poor solvent such as hexane.[12] In contrast, long-time relaxation of shorter QT-amide molecules clearly reflects the *inter*molecular transformations that are much slower than *intra*molecular processes due to entropy. Similar "assisted planarization" has been described previously by Janssen at. al.[13] for substituted oligothiophenes. In that case the aggregation (and planarization) was driven by the $\pi$-stacking interaction. QT-amides aggregate due to the combination of $\pi$-stacking interactions and hydrogen

(11) Salaneck, W. R.; Inganäs, O.; Themans, B.; Nilsson, J. O.; Sjögren, B.; Österholm, J. E.; Bredas, J. L.; Svensson, S. *J. Chem. Phys.* **1988**, *89*, 4613. Faid, K.; Frechette, M.; Ranger, M.; Mazerolle, L.; Levesque, I.; Leclerc, M.; Chen, T. A.; Rieke, R. D. *Chem. Mater.* **1995**, *7*, 1390. Yue, S.; Berry, G. C.; McCullough, R. D. *Macromolecules* **1996**, *29*, 933. Langeveld-Voss, B. M. W.; Janssen, R. A. J.; Christiaans, M. P. T.; Meskers, S. C. J.; Dekkers, H. P. J. M.; Meijer, E. W. *J. Am. Chem. Soc.* **1996**, *118*, 4908. Levesque, I.; Leclerc, M. *Chem. Mater.* **1996,** *8*, 2843−2849. Levesque, I.; Bazinet, P.; Roovers, J. *Macromolecules* **2000**, *33*, 2952. Schenning, A. P. H. J.; Kilbinger, A. F. M.; Biscarini, F.; Cavallini, M.; Cooper, H. J.; Derrick, P. J.; Feast, W. J.; Lazzaroni, R.; Leclere, Ph.; McDonell, L. A.; Meijer, E. W.; Meskers, S. C. J. *J. Am. Chem. Soc.* **2002**, *124*, 1269.

(12) Kiriy, N.; Jähne, E.; Adler, H.-J.; Schneider, M.; Kiriy, A.; Gorodyska, G.; Minko, S.; Jehnichen, D.; Simon, P.; Fokin, A. A.; Stamm, M. *Nano Lett.* **2003**, *3*, 707.

(13) Apperloo, J. J.; Janssen, R. A. J.; Malenfant, P. R. L.; Frechet, J. M. J. *Macromolecules* **2000**, *33*, 7038−7043.

bonding.[14] The important role of hydrogen bonding can be deduced from the spectral data: when the formation of hydrogen bonds is impossible (for QT-aniline, or for QT-amide in the presence of polar solvents) the aggregation (and planarization) does not occur.

**QT-aniline and QT-amide Films.** The morphologies of QT-aniline and QT-amide films were studied by atomic force microscopy (AFM).[15] QT-amide displays excellent film-forming properties and forms homogeneous layers that fully cover surfaces. As an example, Figure 4a shows a smooth, featureless film of QT-amide deposited by spincoating from THF solution onto a Si wafer.

Similar films were obtained by spincoating of QT-aniline (not shown). No improvement of the morphology of the QT-aniline films was observed after annealing at different temperatures. In contrast, the annealing of QT-amide films during 3 h at 180 °C leads to the formation of terrace structures with uniform steps of about 1.5 nm in height (Figure 4b−e). X-ray diffraction (XRD) studies of QT-aniline and QT-amide powders reveal their crystalline nature. Unfortunately, we did not succeed in growing single crystals of these materials; therefore their exact molecular structure is still unknown. XRD measurements of oligomer films in transmission mode were also performed.

No structural organization could be deduced from X-ray analysis of "as deposited" QT-aniline and QT-amide films (Figure 5a), as well as for the annealed QT-aniline film. In contrast, QT-amide films undergo a dramatic transformation upon annealing, as confirmed by XRD. The X-ray diffractogram of QT-amide films annealed during 1 h at 120 °C exhibit two reflections with moderate intensity at $2\theta = 4.63°$ ($d$ spacing 19.05 Å), and 5.53° (15.97 Å). Longer annealing time, and/or higher annealing temperature (180 °C) led to a disappearance of the low-angle reflection and a drastic increase in the intensity of the reflection at 5.63° (15.69 Å). This value is close to the thickness of terraces observed by AFM and might correspond to the distances between closely packed oligomer molecules with interdigitated side chains, as shown in Figure 5b. A similar spacing of about 15 Å was previously found in the X-ray diffractogram of a polyazomethine containing hexyl-substituted oligothiophenes. The observation was also attributed to the formation of a layered structure with interdigitated side chains.[16] The spacing of 19.05 Å, obviously, presents an intermediate phase with less-dense packing of the molecules. Absence of all other reflections (or their relative weakness as compared to the strong 15.69 Å reflection) in the diffractogram of QT-amide films as compared to the XRD-spectra of the QT-amide powder indicates a high degree of preferential orientation of the oligomer molecules.

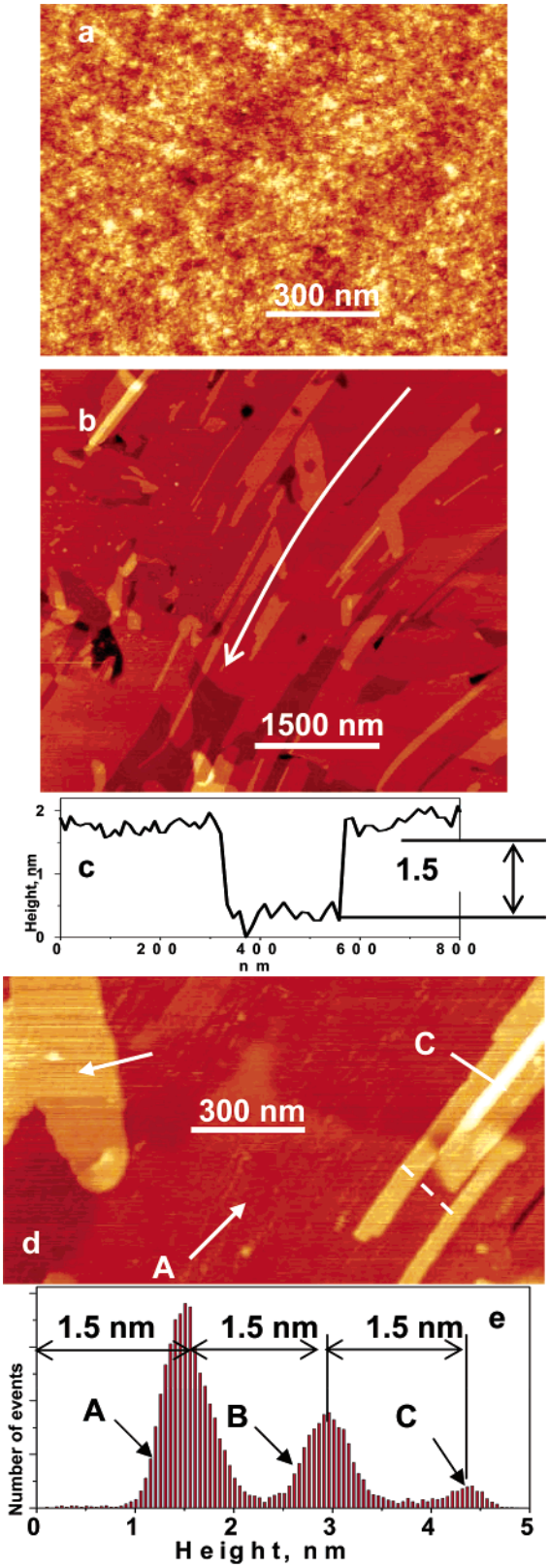


**Figure 4.** AFM images of QT-amide (a, b, d) films: "as deposited" by the spincoating from THF solution (a); the same film after the annealing at 180 °C for 3 h (b, d). The arrow in the image (b) shows the most probable direction of the flow derived from the alignment of terraces. Cross-section (c), and histogram of heights distribution of the image (d) reflect a formation of terrace structures with uniform steps of about 1.5 nm (e).

(14) Schenning, A. P. H. J.; Peeters, E.; Meijer, E. W. *J. Am. Chem. Soc.* **2000,** *122,* 4489. Brunsveld, L.; Zhang, H.; Glasbeek, M.; Vekemans, J. A. J. M.; Meijer, E. W. *J. Am. Chem. Soc.* **2000,** *122,* 6175. Brunsveld, L.; Folmer, B. J. B.; Meijer, E. W.; Sijbesma, R. P. *Chem. Rev.* **2001,** *101,* 4071.

(15) Tsukruk, V. V.; Reneker, D. H. *Polymer* **1995**, *36*, 1791−1808. Minko, S., Kiriy, A., Gorodyska, G., Stamm, M. *J. Am. Chem. Soc.* **2002**, *124*, 3218. Minko, S.; Kiriy, A.; Gorodyska, A.; Stamm, M. *J. Am. Chem. Soc.* **2002**, *124*, 10192. Kiriy, A.; Gorodyska, G.; Minko, S.; Jaeger, W.; Stepanek, P.; Stamm, M. *J. Am. Chem. Soc.* **2002**, *124*, 13454. Kiriy, A.; Gorodyska, G.; Minko, S.; Jaeger, W.; Stepanek, P., Stamm, M. *J. Am. Chem. Soc.* **2003**, *124*, 13454.

(16) Olinga, T. E.; Destri, S.; Botta, C.; Pozio, W.; Consonni, R. *Macromolecules* **1998**, *31*, 1070.

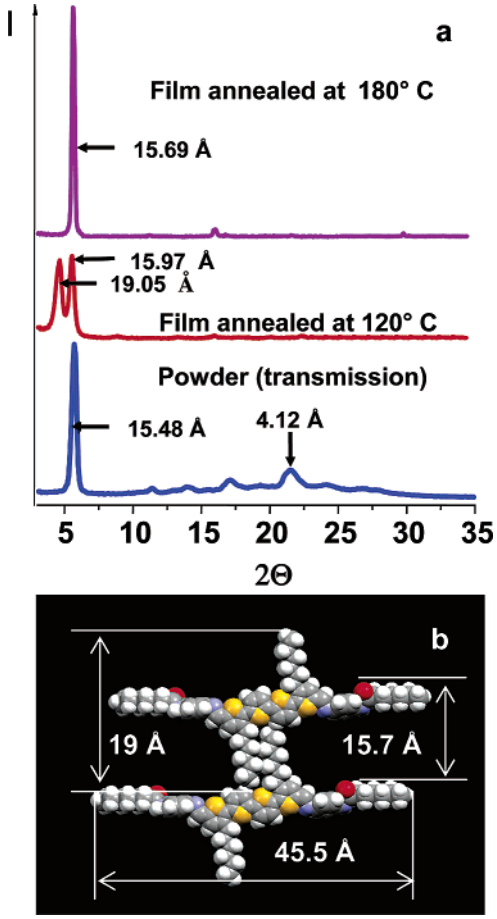


**Figure 5.** X-ray diffractograms of powder (bottom line) and 100-nm thick QT-amide film annealed at 120 °C during 1 h (middle line), the same film annealed at 180 °C for 3 h (top line) (a); proposed orientation of QT-amide molecules in the films (b).

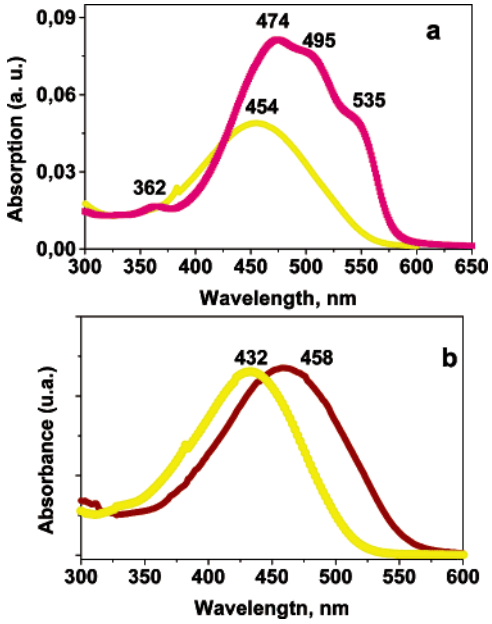


**Figure 6.** UV−vis absorption spectra of: (a) "as-deposited" by spincoating QT-amide film (yellow line), and the same film after the annealing at 180 °C for 3 h; similar spectra was also obtained when "as-deposited" QT-amide film was exposed in methanol vapor; (b) QT-aniline solution in chloroform (yellow line), and QT-aniline film deposited by spincoating from chloroform (red line).

Important information can be extracted from the UV−vis data of oligomer films. Both QT-aniline and "as deposited" QT-amide films display broad featureless spectra with $\lambda_{max}$ about 450 nm that reflects twisted conformation and a rather disordered state (Figure 6).

Upon annealing of the QT-amide films considerable red shift of the UV−vis absorption maximum (from $\lambda_{max} = 448$ nm to $\lambda_{max} = 500$ nm) is observed, along with the appearance of the fine structure and a drastic increase in the overall absorption intensity (extinction coefficient). This observation confirms that significant structural reorganization takes place during annealing of the QT-amide film. The same transformations of UV−vis spectra were also observed when the "as deposited" films were exposed to methanol vapor for a few minutes. A similar approach, termed "vapor annealing", was recently applied for structural modification of other polymer films.[17]

Although no clear signs of the molecular order for "*as deposited*" QT-amide films are observed by AFM, UV−vis and XRD measurements, the terraces observed *after annealing* show an important alignment that originates from the spincoating procedure (Figure 4). This fact strongly supports the argument that initial spincoating leads to a preorganization of QT-amide molecules (undetectable by AFM, UV−vis, and XRD). Upon annealing, the long-range order is developed. Although the exact nature of this phenomenon is still unknown, we believe that hydrogen bonding plays an important role. We hypothesized that fast evaporation of the solvent during spincoating leads to the formation of the viscous gel-like network, stable due to the hydrogen bonding and $\pi$-stacking interactions, that is then preorganized by the shear field experienced during the spincoating process.[5,18] Taking the great influence of the macroscopic orientation in organic semiconductor films on their electrical properties, this finding could be of significant importance for further progress of organic FETs.

It was previously shown that the presence of basic nitrogen atoms in the polyazomethine structure increases the affinity towards protons and various Lewis acids. This was reflected in remarkable ionochromic effects attributed to the ion-coordination-induced coplanarization of the polymer backbones.[7,9,19] Similar transformations of QT-amide films were monitored by UV−vis spectroscopy. Particularly, we found that exposure of the QT-amide film for a few seconds to HCl vapor changes the color of the film from red to blue and shifts the absorption maximum from 454 to 565 nm (Figure 7). Further exposure of the film to ammonia vapor reverses the effect to the initial state. The ammonium chloride formed during the protonation and deprotonation steps either remains trapped in the film or is removed by air scavenging. Similar transformations were also observed in QT-aniline films (UV−vis data not shown).

(17) Sidorenko, A.; Tokarev, I.; Minko, S.; Stamm, M. *J. Am. Chem. Soc.* **2003**, *125*, 12211. Fukunaga, K.; Elbs, H.; Magerle, R.; Krausch, G. *Macromolecules* **2000**, *33*, 947.

(18) Liu, P.; Shirota, Y.; Osada, Y. *Polym. Adv. Technol.* **2000**, *11*, 512.

(19) Zotti, G.; Randi, A.; Destri, S.; Pozio, W.; Schiavon G. *Chem. Mater.* **2002**, *14*, 4550.

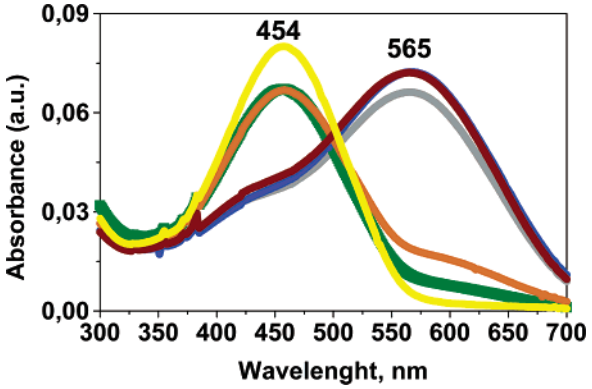


**Figure 7.** Evolution of UV−vis absorption spectra of the same QT-amide film after sequential exposures in HCl and then in $NH_3$ vapors: "as deposited" by spincoating (yellow line, $\lambda_{max} = 454$ nm); after a few-second exposure in HCl vapors (brown, blue and gray lines, $\lambda_{max} = 565$ nm); after a few-second exposure in $NH_3$ vapors (green and orange lines, 454 nm).

**Charge Carrier Mobility.** The intrinsic charge transport properties of QT-aniline and QT-amide were determined by the pulse-radiolysis time-resolved microwave conductivity (PR-TRMC) technique. Charge carriers are produced in a powder sample by irradiation with a short pulse (150 ns) of high-energy (10 MeV) electrons, and the resulting change in conductivity is monitored with R-band microwaves (26−40GHz). The technique has been described in detail in the literature by Warman et al.[20a] The setup used for the experiments reported here have been described by Krebs and Jorgensen.[20] The PR-TRMC method does not rely on electrical contacts being made and thus avoids barrier problems between electrodes and sample, at domain boundaries and between crystallites. The values obtained for the charge carrier mobilities should thus be considered as the maximum trap free mobility within an ordered domain. The sum of charge carrier mobilities of QT-amide was determined to be $\Sigma\mu_{min} = 1 \times 10^{-2}$ cm$^2$ V$^{-1}$ s$^{-1}$ (Figure 8). The half-life of the carriers is of the order of 10 $\mu$s and we ascribe this relatively long lifetime to the efficient formation of a low-dimensional structure where the alkyl groups form an insulating barrier to recombination of charge carrier pairs. This behavior has been reported previously using the same technique for studies of charge carrier mobilities and lifetimes of discotic liquid crystals.[21]

This value is equal to the PR-TRMC mobility of $\alpha,\omega$-DH6T[4] and other semiconductors successfully used in FET.[11] In contrast, QT-aniline exhibits a poor PR-TRMC mobility below the detectable limit. The measurements of the field effect mobility for QT-amide is in progress.

## Conclusions

In this paper we have described the synthesis and characterization of two thiophene-based azomethines designed to increase solubility, improve self-assembly properties, and exhibit good charge carrier mobility. We found that incorporation of azomethine and amide moiety in the $\alpha,\omega$-position, and hexyl chains in $\beta$-position of the quaterthiophene, considerably improves the self-assembly properties without affecting the solubility. The self-assembly of azomethine oligomers with and without amide moieties was monitored by UV−vis, XRD, and AFM. Although no conformational changes of QT-aniline was observed upon addition of hexane to the solution in THF, the addition of hexane to QT-amide solution induced a red shift of $\lambda_{max}$ and the appearance of the fine structure ascribed to vibronic transitions. The concentration dependence of the solvatochromism gives strong support for the *inter*molecular origin of this effect and clearly indicated that the planarization of the oligomer backbone was induced by the aggregation. Although no clear signs of the molecular order for various QT-aniline films were observed by AFM, UV−vis, and XRD measurements, the QT-amide annealed film displayed an important molecular and macroscopic orientation. QT-aniline showed PR-TRMC below the detectable limit; the PR-TRMC mobility of the QT-amide is comparable with the PR-TRMC mobilities of the best organic semiconductors. All these significant differences in properties of related compounds can be attributed to the hydrogen bonding developed between the QT-amide molecules that induces self-assembly.

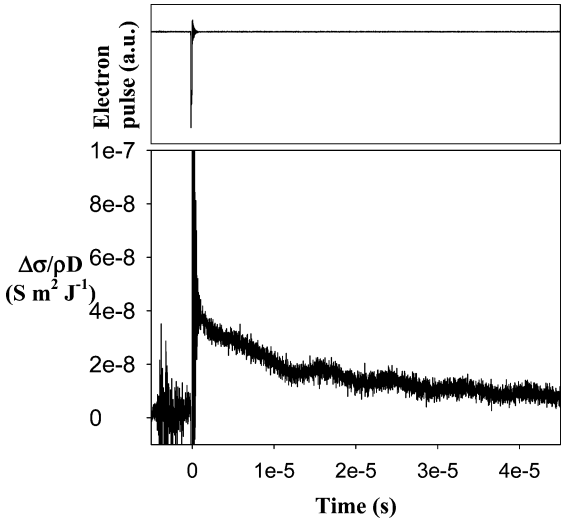


**Figure 8.** Dose-normalized conductivity change shown along with the corresponding minimum sum of charge carrier mobilities based on a pair formation energy of 25 eV and a survival probability of 1 taken at the end-of-pulse.

## Experimental Section

**General.** All chemicals were purchased from Aldrich and used as received. $^1$H and $^{13}$C NMR spectra were recorded on Bruker DRX-500 spectrometer at frequencies of 500.13 MHz ($^1$H) and 125.76 MHz ($^{13}$C) with tetramethylsilane as an internal standard. UV−vis measurements were carried out using a Perkin-Elmer UV/vis Spectrometer Lambda 19. MALDI-TOF was performed on a Bruker Biflex IV mass-spectrometer. IR spectra were recorded with a Brucker IFS 48 FTIR spectrometer. For AFM measurements we used a Multimode AFM instrument (Digital Instruments, Santa Barbara) operating in the tapping mode. Silicon tips with the radius of 10−20 nm, the spring constant of 0.3 N/m and the resonance frequency of 250−300 kHz. XRD diagrams of powders were recorded in transmission using an X-ray diffractometer P4 (Siemens AG Karlsruhe) with Cu−K$\alpha$ radiation (monochromatization by primary graphite crystal); primary pinhole

(20) (a) Warman, J. M.; Gelinck, G. H.; de Haas, M. P. *J. Phys.: Condens. Matter* **2002**, *14*, 9935. (b) Krebs, F. C.; Jorgensen, M. *Macromolecules* **2003**, *36*, 4374.

(21) Schouten, P. G.; Warman, J. M.; de Haas, M. P.; Fox, M. A.; Pan, H.-L. *Nature* **1991**, *353*, 736−737.

Ø = 0.5 mm; detector distance 12 cm; measuring time $\Delta t$ = 360 s (accumulation). XRD diagrams of films were recorded in reflection using XRD 3003 (Seifert-FPM Freiberg/Sa.) (monochromatization by primary multilayer system).

**Sample Preparation.** Highly polished Si wafers (obtained from Wacker-Chemitronics) were first cleaned in a ultrasonic bath 3 times for 5 min with dichloromethane, placed in cleaning solution (prepared from $NH_4OH$ and $H_2O_2$) for 1 h, and finally rinsed several times with Millipore water (18 MQxcm). Oligomers were deposited onto a Si wafer by spin-coating (2000 rot/min) from 2 to 5% solution in THF.

*3,3‴-Dihexyl-2,2′;5′,2″;5″,2‴-tetrathienyl (DHQT).* DHQT was obtained as previously described.[10]

*5,5‴-Diformyl-3,3‴-dihexyl-2,2′;5′,2″;5″,2‴-quaterthiophene (QTDA).* To prepare the Vilsmeier reagent a solution of 3.29 g (0.0215 mol) of $POCl_3$ and 1.7 g (0.0233 mol) of DMF in 25 mL absolute $CH_2Cl_2$ were stirred for 2 h at room temperature. This solution was added to 4.98 g (0.01 mol) of DHQT dissolved in 20 mL $CHCl_3$. The resulting mixture was stirred at room temperature overnight, neutralized with cold 1N $Na_2CO_3$ solution and then extracted with $CHCl_3$. The organic layer was dried over $MgSO_4$ and evaporated. The residue was purified by crystallization from $CHCl_3$-hexane mixture and 4.1 g (74%) of QTDA was obtained. $^1$H NMR ($CDCl_3$, ppm, TMS): $\delta$ 9.80 (s., CH=O); $\delta$ 7.56 (s., 1H); $\delta$ 7.18−7.15 (m., 2H); $\delta$ 2.78, (t., $J$ = 7.8, 2H); $\delta$ 1.70−1.63 (m., 2H); $\delta$ 1.41−1.37 (m., 2H); $\delta$ 1.33−1.23 (m., 4H); $\delta$ 0.88 (t., $J$ = 6.9, 3H). $^{13}$C NMR ($CDCl_3$, ppm, TMS): $\delta$ 182.378; 140.527; 140.445; 140.335; 138.909; 138.117; 134,402; 128.181; 124.648; 31.519; 30.092; 29.384; 29.066; 22.509; 14.012. UV−vis ($CHCl_3$): $\lambda_{max}$ = 424 nm; mp = 125.8 °C.

*5,5‴-Diphenyliminomethyl-3,3‴-Dihexyl-2,2′;5′,2″;5″,2‴-tetrathienyl (QT-aniline).* Solutions of 1.1 g (0.002 mol) of QTDA in 10 mL of $CHCl_3$ and 0.74 g (0.008 mol) of aniline in 10 mL of absolute ethanol were gently refluxed overnight. The reaction mixture was concentrated until the crystal precipitated. The powder was filtered, washed, and then recrystallized in ethanol−$CHCl_3$ mixture. Yield: 1.24 g, 91%. $^1$H NMR ($CDCl_3$, ppm, TMS): $\delta$ 8.47 (s., CH-d=N); $\delta$ 7.38 (m., 2H−c); $\delta$ 7.30 (s., 1H−e); $\delta$ 7.21−7.22−7.17 (m., 5H−a,b,f,g); $\delta$ 2.81, (t., $J$ = 7.5, 2H); $\delta$ 1.69 (m., 2H); $\delta$ 1.55−1.33 (m., 6H); $\delta$ 0.88 (t., $J$ = 5.6, 3H). $^{13}$C NMR ($CDCl_3$, ppm, TMS): $\delta$ 152.48; 151.34; 140.05; 139.94; 137.44; 135.47; 135.13; 129.14; 127.32; 126.05; 124.36; 121.04; 119.77; 31.64; 30.29; 29.50; 29.18; 22.69; 14.10. *m/e* 704 ($M^{+\bullet}$). FTIR (KBr): 2921 (C−H-bend), 1578 (C=N-stretch), 1435 (C−C ring stretch). UV−vis ($CHCl_3$): $\lambda_{max}$ = 432 nm; mp = 111.8 °C.

*Heptanoic Acid (4-aminophenyl)amide (PDA-Ac).* 10.8 g (0.1mol) of *p*-phenylenediamine and 9 g of pyridine were dissolved in 500 mL of dry THF and cooled to −40 °C. A solution of 14.85 g (0.1mol) of heptanoyl chloride in 100 mL of THF was added dropwise under vigorous stirring. After the addition of heptanoyl chloride, the reaction mixture was allowed to warm to room temperature and stirred overnight. The mixture was concentrated in a vacuum to 100 mL, 100 mL of hexane was added, and the resulting powder of pyridine chlorohydrate and bis-acylated *p*-phenylenediamine was filtered. The resulting solution was washed with water and dried over $MgSO_4$. The crude PDA-Ac was obtained after the evaporation of the solvent and purified by flash chromatography followed by the crystallization from the $CHCl_3$−hexane mixture (1/1 v/v). Yield: 7.7 g, 35%. $^1$H NMR ($CDCl_3$, ppm, TMS): $\delta$ 7.26 (d., $J$ = 8.6, 2H); $\delta$ 6.23 (d., $J$ = 8.6, 2H); $\delta$ 2.29, (t., $J$ = 7.5 2H); $\delta$ 1.68 (d.d., $J_1$ = 7.2, $J_2$ = 7. 5, 2H); $\delta$ 1.37−1.28 (m., 6H); $\delta$ 0.88 (t., $J$ = 6.8, 3H). FTIR (KBr): 3280 (N−H-stretch), 2926 (C−H-bend), 1648 (C=O-stretch), 1533 (C−N-stretch, amid II).

*Heptanoic Acid [4-({5‴-[(4-heptanoylamino-phenylimino)-methyl]-3,3‴-dihexyl-[2,2′;5′,2″;5″,2‴]quaterthiophen-5-ylmethylene}-amino)-phenyl]-amide (QT-amide).* Solutions of 1.1 g (0.002 mol) of QTDA in 10 mL of $CHCl_3$ and 0.74 g (0.008 mol) of PDA-Ac in 10 mL of absolute ethanol were gently refluxed overnight until orange crystals precipitated out. The powder was filtered, washed, and then crystallized from the ethanol−THF mixture (1/2 v/v). Yield: 1.16 g, 85%. $^1$H NMR (DMSO-d6, ppm, TMS): $\delta$ 9.48 (s., NH-a); 8.46 (s., CH-d=N); $\delta$ 7.57 (d., 2H−b, J = 8.5); $\delta$ 7.27 (s., 1H−e); $\delta$ 7.16−7.10 (m., 4H−c,f,g); $\delta$ 2.73, (t., J = 7, 2H); $\delta$ 2.28, (t., J = 7, 2H); $\delta$ 1.6 (m., 4H); $\delta$ 1.35−1.25 (m., 10H); $\delta$ 0.88 (m., 6H). $^{13}$C NMR (DMSO-d6, ppm, TMS): 171.10; 150.55; 145.15; 140.03; 139.62; 137.64; 136.34; 135.07; 134.40; 133.72; 127.06; 124.41; 121.09; 119.58; 36.46; 31.00; 30.96; 29.56; 28.81; 28.45; 28.33; 25.01; 21.95; 21.90; 13.71; 13.69. m/e 958 ($M^{+\bullet}$). FTIR (KBr): 3300−3100 (N−H-stretch), 2922 (C−H-bend), 1700 (C=O-stretch), 1607 (C=N-stretch), 1530 (C−N-stretch, amid II), 1448 (C−C ring stretch). UV−vis ($CHCl_3$): $\lambda_{max}$ = 442 nm; mp = 202.4 °C.

**Acknowledgment.** The authors thank Dr. E. Jähne for helpful discussions and Dr. D. Kukling for MALDI-TOF measurements. We are grateful for the financial support provided by Deutsche Forschungsgemeinschaft (Project DFG-Sachb. AD 119/6-1 and DFG/CNRS German-French bilateral program, STA 324/13).

CM049688V